

## Progress in cleaning and wet processing for kesterite thin film solar cells

Bart Vermang<sup>1,2,a</sup>, Aniket Mule<sup>1,3</sup>, Nikhil Gampa<sup>1,4</sup>, Sylvester Sahayaraj<sup>1,2</sup>,  
Samaneh Ranjbar<sup>1,5</sup>, Guy Brammertz<sup>1,6</sup>, Marc Meuris<sup>1,6</sup>  
and Jef Poortmans<sup>2,6</sup>

<sup>1</sup> imec division IMOMECE – partner in solliance, Diepenbeek, Belgium

<sup>2</sup> Department of Electrical Engineering, KU Leuven, Heverlee, Belgium

<sup>3</sup> Department of Mechanical and Process Engineering, ETH Zurich, Zurich, Switzerland

<sup>4</sup> Department of Engineering, Université Claude Bernard Lyon 1, Villeurbanne, France

<sup>5</sup> Department of Physics, Universidade de Aveiro, Aveiro, Portugal

<sup>6</sup> Inst. for Material Research (IMO) Hasselt University – partner in Solliance, Diepenbeek, Belgium

<sup>a</sup> bart.vermang@imec.be

**Keywords:** Photovoltaics, PV, thin film, kesterite, CZTS, wet processing, alkali, surface, cleaning, etching, passivation, chalcopyrite, CIGS.

### Kesterite solar cells, the new kid on the block

The photovoltaic module manufacturing market is booming and presently dominated by Si modules, but also thin film (TF) photovoltaics (PV) remain very interesting due to their high potential for new applications and markets. TF PV can be completely processed on large rigid (e.g. glass) or flexible and thus lightweight substrates (e.g. steel) by use of monolithic integration (P1, P2 and P3 scribes). This is an interconnection technology that leads to a dark smooth appearance and is free of classic size limitations. Hence, such modules bring many exciting architectural choices with regards to size, shape, color and function; all important characteristics for building integrated PV (BIPV), a key future market. Additional advantages of TF PV are (i) the high energy yield and outstanding outdoor performance, (ii) the low energy consumption, short energy payback time and minimized material consumption, (iii) its proven reliability, (iv) the high productivity at the GW production level, and (v) the low production costs [1].

Cadmium telluride (CdTe) and copper indium gallium selenide/sulfide (CIGS) are the two main TF PV technologies, together they represent the largest TF PV market share and the highest energy conversion efficiencies, but unfortunately also toxicity and abundance concerns. Indeed, two thirds of the TF PV market is provided by the two largest TF companies: First Solar (CdTe) and Solar Frontier (CIGS). Both companies are very successful in the development of their technologies, as demonstrated by their presence in the TF PV world record efficiency charts. These up-to-date record efficiencies are 21.0 % at cell level, as obtained by First Solar and Solibro (CIGS), and respectively 18.6 % (obtained by First solar) or 17.5 % (obtained by Solar Frontier) at module level. However, these technologies also embody clear toxicity (the use of poisonous Cd in CdTe PV) and abundance (the use of rare elements In and Ga in CIGS PV) concerns [2].

Copper zinc tin selenide/sulfide (CZTS) is a non-toxic and earth-abundant alternative with great potential, but material and device improvements are essential. A novel (first solar cell developed in 1996) TF PV material is CZTS, which is derived from the related CIGS compound by substitution of In and Ga for Zn and Sn. This isoelectronic substitution produces a material with many similar properties of the parent compound. Indeed, the CZTS kesterite and CIGS chalcopyrite structures are known to be associated, where the advantage of CZTS lays in its composition of non-toxic and abundant materials. At present, top conversion efficiencies for small-area CIGS solar cells are typically above 20 % (e.g. NREL, ZSW, HZB, EMPA, Solibro, Solar Frontier, etc.), whereas CZTS solar cells are limited to efficiencies slightly above 10 % (e.g. IBM, Imec, IREC, Solar Frontier,

etc.). The main reason is that the CZTS technology is not as mature, where many difficulties need to be addressed to increase electrical performance. Typical issues are secondary phase formation, fluctuating potentials, reproducibility and stability, and also cell architecture [3,4]. A typical kesterite solar cell structure is shown in Fig. 1, as taken from [5].

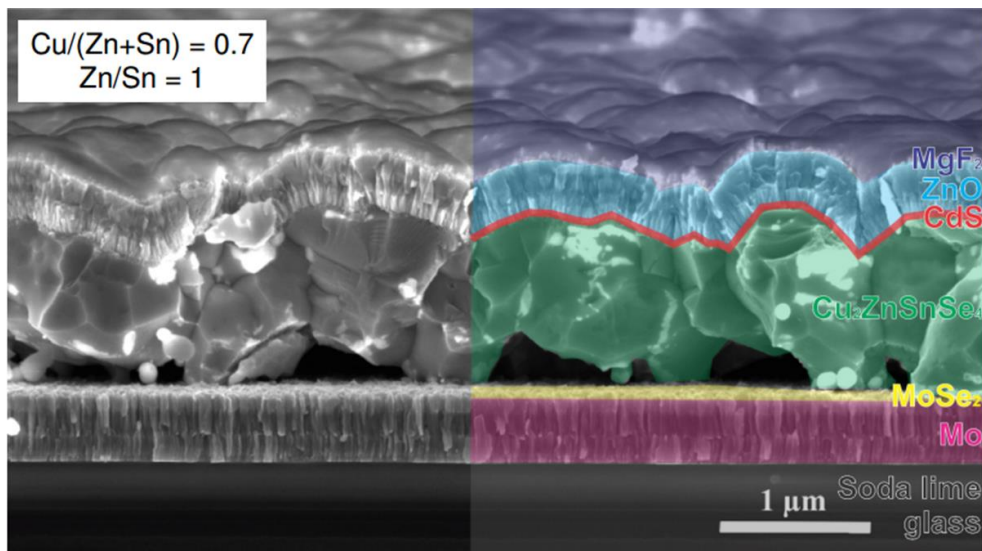


Figure 1: Scanning electron microscopy cross-section image of a typical kesterite solar cell, where the different layers are highlighted in different colors (taken from [5]).

**In this work**, three new processing steps – which are well-known to be beneficial for CIGS solar cell processing – are developed, optimized and implemented in CZTS solar cells. These three steps are known to improve the CIGS absorber layer by (i) the incorporation of alkali metals, (ii) cleaning of its surface, or (iii) the electrical passivation of its surface. (i) The incorporation of sodium (Na) and potassium (K) in and its positive influence on CIGS solar cells is well-studied. Na is reported to influence crystallinity, hinder inter-diffusion of In and Ga, change preferential crystal orientation, and increase the free carrier concentration of the CIGS absorber [6]. And the presence of K is shown to increase junction depth and band-gap (higher Ga content), and enhance passivation (grain boundaries and donor-like defects) [7]. (ii) It has been proven that both potassium cyanide (KCN) and ammonium sulfide (AS =  $(\text{NH}_4)_2\text{S}$ ) treatments are successful in removing detrimental secondary phases in CIGS, where the focus is on the removal of  $\text{Cu}_x\text{Se}$  – which is known to increase the shunt conductance. Both wet treatments are found to selectively etch  $\text{Cu}_x\text{Se}$  phases, but lower etching rates are observed for the AS solution. Nevertheless, the AS treatment is shown to passivate the CIGS surface by incorporation of sulfur (as proven by an increase in minority carrier lifetime), which results in a solar performance enhancement [8]. (iii) Rear and front surface passivation approaches have already been introduced in CIGS solar cells. Therefore passivation layers are combined with nano-sized point openings, where the purpose of the passivation layer is to reduce charge carrier recombination at the CIGS surface, while the point openings serve as electrical contacts. Various approaches have been reported:  $\text{Al}_2\text{O}_3$  rear surface passivation [9], and the spray-ILGAR<sup>®</sup> or SALT front surface passivation methodologies [10,11].

### Advances in cleaning and wet processing for kesterite solar cells

Fig. 1(a) shows the effect of Na and K on CZTS absorber layer quality. In standard kesterite solar cell processing soda lime glass (SLG) substrates are used, wherefore it is known that Na (and very little K) diffuses – in an uncontrolled manner – from the glass into the CZTS absorber layer.

Therefore, in the case of alkali treated samples these SLG substrates have been covered with a (silicon nitride) barrier layer to prevent this diffusion process from the SLG. Fig. 1(a) gives an overview of alkali treated CZTS layers grown on such SLG substrates with barrier layer. This figure gives an estimation of the average minority carrier lifetime of simplified devices, as obtained by time-resolved photoluminescence (TRPL). This minority carrier lifetime is derived using an exponential fit to the PL decay curve, where the slowest decay time is reported to be related to the low injection minority carrier lifetime. Hence, this figure clearly shows the potential absorber layer quality improvement in case of a well-controlled supply of Na and K. The effects of Na and K on CZTS solar cells are not yet well-understood, but other initial studies indicate a positive impact in both cases. Besides affecting the size of grains, Na has been shown to mainly decrease the defect and trap densities within the absorber bulk and at interfaces. The presence of K has been related to an increase in bulk crystallinity (and enhance the (112) preferred orientation), and a reduction in zinc sulfide (ZnS) secondary phase formation. Note that – amongst the other alkali metals – also Li seems to be a promising dopant, as far as optoelectronic properties are concerned [12].

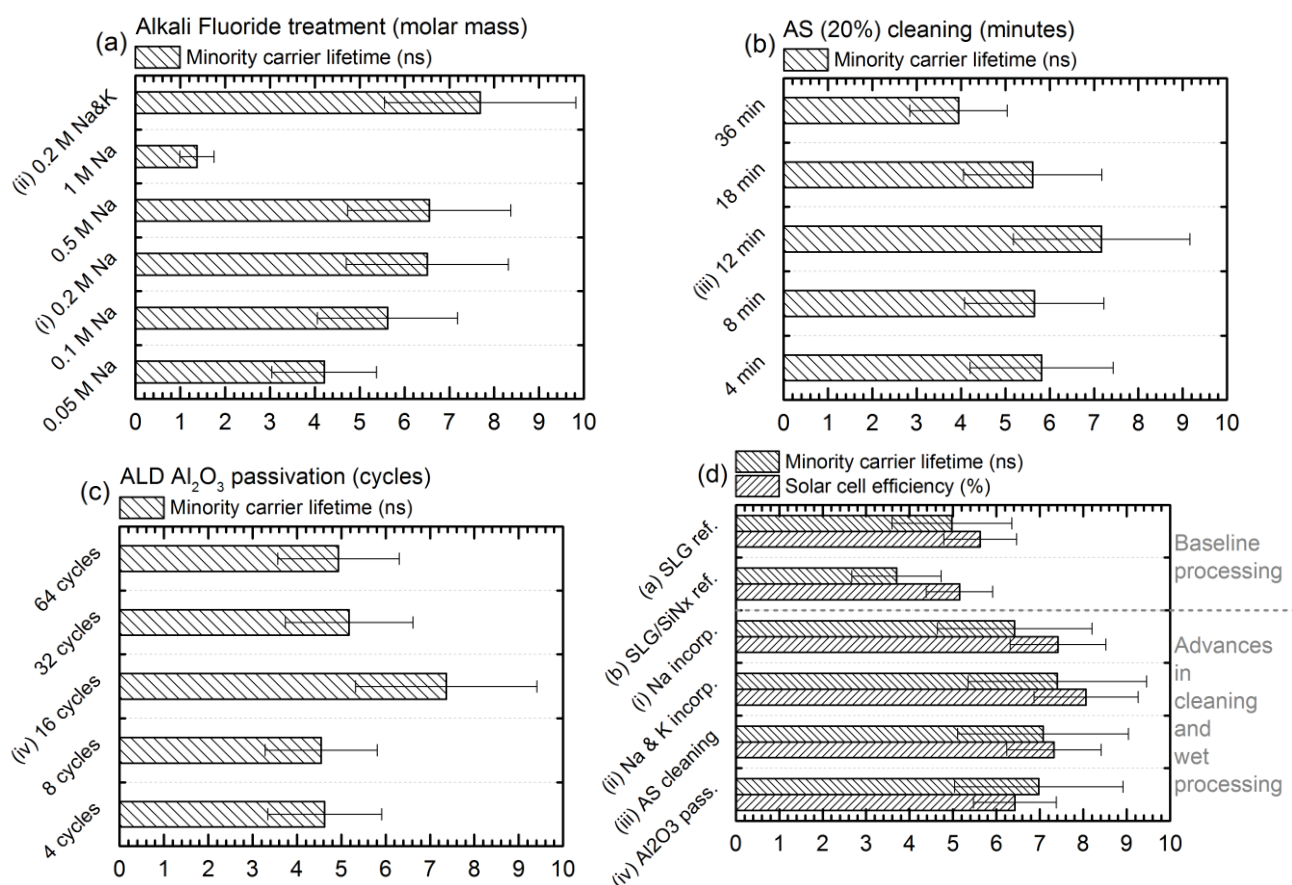


Figure 2: Average minority carrier lifetime for simplified kesterite devices, (a) grown on soda lime glass (SLG) / barrier-layer (thus without the supply of Na and K) substrates combined with an additional alkali (Na and/or K) fluoride treatment step, or (b) or (c) grown on SLG substrates combined with an extra surface cleaning ((NH<sub>4</sub>)<sub>2</sub>S) or passivation (Al<sub>2</sub>O<sub>3</sub>) step, respectively. (d) Average minority carrier lifetime and cell efficiency for complete kesterite solar cells fabricated on the same substrates and using the optimized processing steps as used in (a), (b) and (c).

Fig. 1(b) shows the effect of AS cleaning on CZTS surface quality. At present, KCN chemical etching is the standard method to remove secondary phases from the surface of the kesterite crystals, which is one of the major CZTS challenges. As compared to CIGS, there is only limited control of the composition and microstructure in the fabrication of CZTS materials. Hence, various secondary phases, such as Zn(S,Se), Cu<sub>x</sub>(S,Se), Sn(S,Se)<sub>x</sub> or Cu<sub>2</sub>Sn(S,Se)<sub>3</sub>, are typically formed during the

processing of the absorber layer and eventually hinder the electrical performance of solar cell devices. The KCN treatment is found to clean the CZTS absorber surface from most of these secondary phase, and consequently became a characteristic kesterite solar cell processing step. On the one hand, standard KCN (5 wt% in aqueous KOH) immersion of the CZTS absorber up to 2 minutes appears to etch away most of these secondary phases. On the other hand, longer KCN etching times does result in the systematic damage of the CZTS surface [13]. A similar optimum is seen for 12 minutes of AS surface cleaning, as is shown in Fig. 1(b). The advantage of AS as compared to KCN, would be its safety, less toxic nature and potential to passivate the CZTS surface by incorporation of sulfur [8].

Fig. 1(c) shows the potential of Al<sub>2</sub>O<sub>3</sub> passivation on the CZTS interface quality. Recently, capacitance-voltage profiling and quantum efficiency measurements have revealed that Al<sub>2</sub>O<sub>3</sub> can lead to reduced interface recombination and a wider depletion width in kesterite solar cells [14]. In addition, the Al<sub>2</sub>O<sub>3</sub> layer may also passivate pinholes and grain boundaries [15]. In this work, very thin Al<sub>2</sub>O<sub>3</sub> front surface passivation layers are grown on a rough and unfavorably terminated CZTS surface, by use of atomic layer deposition (ALD). Hence, these layers should (a) be thin enough so that the photo-excited electrons could effectively tunnel through the layer, or (b) have nano-sized openings due to the surface-inhibited growth. Fig. 1(c) shows the positive impact of such Al<sub>2</sub>O<sub>3</sub> passivation layers on the CZTS surface, where the thickness (and surface coverage) of the layers are tuned by varying the amount of ALD cycles. Note that – previously – similar results have been obtained by use of a TiO<sub>2</sub> front surface passivation layer [16], and an Al<sub>2</sub>O<sub>3</sub> rear surface passivation layer with nano-sized point contacts [17].

In Fig. 1(d) the most optimized procedures (in terms of realized minority carrier lifetime) of these Na, Na & K, AS and Al<sub>2</sub>O<sub>3</sub> processing steps are tried in actual CZTS solar cells, to show their full potential. The Na and Na & K incorporation procedures are implemented into CZTS solar cells fabricated on SLG / barrier-layer substrates, while the AS cleaning and Al<sub>2</sub>O<sub>3</sub> passivation procedures are implemented on standard SLG substrates. As a reference, also regular solar cells have been fabricated on both SLG and SLG / barrier-layer substrates. This figure shows that all these novel cleaning and wet processing successfully increase solar cell performance, as compared with the references. Hence, it also supports our approach to use TRPL to screen and optimize new processing steps in a time-efficient manner, before applying them in tangible solar cell devices.

**In summary**, three new processing steps are successfully integrated into CZTS solar cells. For all these novel processing steps an increase in minority carrier lifetime and cell conversion efficiency is measured, as compared to standard kesterite processing. The scientific explanation of these effects is very similar to its CIGS equivalent: the incorporation of alkali metals, AS surface cleaning, and Al<sub>2</sub>O<sub>3</sub> surface passivation leads to electrical enhancement of the CZTS bulk, front surface and reduced front interface recombination, respectively.

## Experimental section

*Baseline kesterite solar cell processing:* Standard kesterite solar cells have a SLG/Mo/CZTS/CdS/i-ZnO:Al/Ni/Al device structure. First, Sn, Zn and Cu metal layers are e-beam evaporated on a standard SLG(/SiN<sub>x</sub>)/Mo substrate. These stacked metal layers are then selenized in a rapid thermal anneal oven in vacuum, where a continuous flow of 10 % H<sub>2</sub>Se in N<sub>2</sub> is supplied. The ramp up speed is 1 °C/s, and the anneal time is 15 minutes at a temperature of about 450 °C. Hence, a pure selenide p-type CZTS absorber layer of about 1 μm is fabricated. Next, two wet steps are performed: a KCN etch (5 wt% in H<sub>2</sub>O), followed by chemical bath deposition of a n-type CdS buffer layer of 50 nm. The n-type front contact is deposited by sputtering: 100 nm of intrinsic ZnO

followed by 400 nm of Al-doped ZnO. Finally, a front contact Ni/Al grid is deposited while cell isolation is made with needle scribing [4].

*Advances in cleaning and wet processing:* (i) *Incorporation of alkali metals:* Alkali metals are spin-coated onto the CZT metal stack (before selenization). First, the fluoride salts of alkali metals are dissolved in water. Next, this solution is spin coated onto the Sn/Zn/Cu metal stack, with a rotational speed of 1000 rpm and an acceleration of 1000 rpm/s<sup>2</sup>, for 6 minutes. Finally, the alkali metals are incorporated into the CZTS layer during the selenization step. In [12] is presented that the alkali metals have effectively diffused into the absorber, and that the diffused quantity is related to the concentration of alkali metal solution, which demonstrates the controllability of the technique. (ii) *Surface etching/cleaning by (NH<sub>4</sub>)<sub>2</sub>S:* The AS treatment uses as-received ammonium sulfide dissolved in water (20 wt%). The SLG/Mo/CZTS samples are dipped into this solution, followed by 2 min of rinsing in deionized water. (iii) *Al<sub>2</sub>O<sub>3</sub> surface passivation:* ALD of Al<sub>2</sub>O<sub>3</sub>, grown at low temperature ( $\leq 150^{\circ}\text{C}$ ), is used as a one-step front surface passivation layer. In addition, this layer is grown on a rough and unfavorably terminated CZTS surface, and thus might lead to non-conformal surface-inhibited growth, also called island growth [18].

*Characterization:* (i) The metallic composition of the studied absorber layers is determined by *X-ray fluorescence (XRF)*. Absorber layers are prepared under Cu-poor ( $[\text{Cu}]/([\text{Zn}]+[\text{Sn}]) \sim [0.7;0.9]$ ) and Zn-rich ( $[\text{Zn}]/[\text{Sn}] \sim [1.0;1.25]$ ) conditions. In such case, the Zn excess is found to form Zn-rich secondary phases mainly located at the grain boundaries and at the free surface of the CZTS grains. In most cases, however, the CZTS layer is found to also contain some residue of the other secondary phases, even if their formation was prevented by using optimal precursor compositions and synthesis conditions [19]. (ii) *TRPL measurements* are acquired with a near infrared compact fluorescence lifetime measurement system. A circular area with 3 mm diameter is illuminated with a 15 kHz, 1.2 ns pulsed 532 nm laser. Hence, the minority carrier lifetime can be derived using an exponential fit to the photoluminescence decay curve (PL intensity as a function of time). The slowest decay time is reported to be the low injection minority carrier lifetime whereas the faster decay time(s) is/are linked to the charge separation time [20]. The minority carrier lifetime (at zero bias voltage) in standard finished kesterite solar cells is of the order of 4.0 to 6.0 ns. (iii) Solar cells are characterized by *illuminated current-voltage (J-V)* using a standard AM1.5G spectrum with an illumination intensity of 1000 W/m<sup>2</sup>. To date, the best kesterite solar cell fabricated at Imec has an efficiency of 10.4 % [21], while the typical baseline efficiency lays in the range of 4.5 to 6.5 %. Note that a MgF<sub>2</sub> anti-reflection coating has been used for the record cell, which is not part of the baseline processing explained above.

## Acknowledgments

This work is funded by the Flemish government (Department Economy, Science and Innovation) and the European Union (Horizon 2020 grant agreement No 640868). B. Vermang acknowledges the financial support of the Flemish Research Foundation FWO (mandate 12O4215N).

## References

- [1] White paper for CIGS thin film solar cell technology, e.g. <http://www.solarpowerworldonline.com/wp-content/uploads/2016/01/CIGS-WhitePaper.pdf>, retrieved June 6<sup>th</sup> (2016).
- [2] M.A. Green, K. Emery, Y. Hishikawa, W. Warta and E.D. Dunlop: Prog. Photovolt: Res. Appl. 24(1) (2016), p. 3–11.

- [3] X. Liu, Y. Feng, H. Cui, F. Liu, X. Hao, G. Conibeer, D.B. Mitzi and M. Green: *Prog. Photovolt: Res. Appl.* 24(6) (2016), p. 879–898.
- [4] G. Brammertz, S. Oueslati, M. Buffière, J. Bekaert, H. El Anzeery, K. Ben Messaoud, S. Sahayaraj, T. Nuytten, C. Köble, M. Meuris and J. Poortmans: *IEEE J. Photovoltaics* 5(2) (2014), p. 486–492.
- [5] G. Brammertz, M. Buffière, S. Oueslati, H. El Anzeery, K. Ben Messaoud, S. Sahayaraj, C. Köble, M. Meuris and J. Poortmans: *Appl. Phys. Lett.* 103 (2013) p. 163904.
- [6] P.M.P. Salomé, H. Rodriguez-Alvarez and S. Sadewasser: *Solar Energy Mater. Solar Cells* 143 (2015), p. 9–20.
- [7] A. Chirilă, P. Reinhard, F. Pianezzi, P. Bloesch, A.R. Uhl, C. Fella, L. Kranz, D. Keller, C. Gretener, H. Hagendorfer, D. Jaeger, R. Erni, S. Nishiwaki, S. Buecheler and A.N. Tiwari: *Nature Materials* 12 (2013), pp. 1107–1111.
- [8] M. Buffière, A.-A. El Mel, N. Lenaers, G. Brammertz, A.E. Zaghi, M. Meuris and J. Poortmans: *Adv. Energy Mater.* 5 (2015), p. 1401689.
- [9] B. Vermang, J.T. Wätjen, C. Frisk, V. Fjällström, F. Rostvall, M. Edoff, P. Salomé, J. Borme, N. Nicoara and S. Sadewasser: *IEEE J. Photovoltaics* 4(6) (2014), p. 1644–1649.
- [10] Y. Fu, N.A. Allsop, S.E. Gledhill, T. Köhler, M. Krüger, R. Sáez-Araoz, U. Blöck, M.Ch. Lux-Steiner and C.-H. Fischer: *Adv. Energy Mater.* 1(4) (2011), p. 561–564.
- [11] P. Reinhard, B. Bissig, F. Pianezzi, H. Hagendorfer, G. Sozzi, R. Menozzi, C. Gretener, S. Nishiwaki, S. Buecheler and A.N. Tiwari: *Nano Lett.* 15(5) (2015), p. 3334–3340.
- [12] A. Mule, B. Vermang, M. Sylvester, G. Brammertz, S. Ranjbar, T. Schnabel, N. Gampa, M. Meuris and J. Poortmans: *Thin Solid Films* XX (2016), under review.
- [13] M. Sylvester, G. Brammertz, B. Vermang, M. Meuris, J. Vleugels and J. Poortmans: *Thin Solid Films* XX (2016), under review.
- [14] M.E. Erkan, V. Chawla and M.A. Scarpulla: *J. Appl. Phys.* 119 (2016), p. 194504.
- [15] Y.S. Lee, T. Gershon, T.K. Todorov, W. Wang, M.T. Winkler, M. Hopstaken, O. Gunawan and J. Kim: *Adv. Energy Mater.* XX (2016), early view, DOI: 10.1002/aenm.201600198.
- [16] W. Wu, Y. Cao, J.V. Caspar, Q. Guo, L.K. Johnson, R.S. Mclean, I. Malajovich and K.R. Choudhury: *Appl. Phys. Lett.* 105 (2014), p. 042108.
- [17] B. Vermang, Y. Ren, O. Donzel-Gargand, C. Frisk, J. Joel, P. Salomé, J. Borme, S. Sadewasser, C. Platzer-Björkman and M. Edoff: *IEEE J. Photovoltaics* 6(1) (2015), p. 332–336.
- [18] S.M. George: *Chem. Rev.* 110 (1) (2010), p. 111–131.
- [19] M. Buffière, G. Brammertz, S. Sahayaraj, M. Batuk, S. Khelifi, D. Mangin, A.-A. El Mel, L. Arzel, J. Hadermann, M. Meuris and J. Poortmans: *ACS Appl. Mater. Interfaces* 7(27) (2015), p. 14690–14698.
- [20] A. Kanevce, D.H. Levi and D. Kuciauskas: *Prog. Photovolt: Res. Appl.* 22 (2014), p. 1138–1146.
- [21] S. Oueslati, G. Brammertz, M. Buffière, H. El Anzeery, O. Touayar, C. Köble, J. Bekaert, M. Meuris and J. Poortmans: *Thin Solid Films* 582 (2015), p. 224–228.